

# FEASIBILITY STUDY OF THE UNIVERSITY OF UTAH TRIGA REACTOR POWER UPGRADE Part I: Neutronics-based study in respect to control rod system requirements and design

by

*Avdo CUTIC, Dongok CHOE, and Tatjana JEVREMOVIC\**

Utah Nuclear Engineering Program, The University of Utah, Salt Lake City, Ut., USA

Scientific paper  
DOI: 10.2298/NTRP1302109C

We present a summary of extensive studies in determining the highest achievable power level of the current University of Utah TRIGA core configuration in respect to control rod requirements. Although the currently licensed University of Utah TRIGA power of 100 kW provides an excellent setting for a wide range of experiments, we investigate the possibility of increasing the power with the existing fuel elements and core structure. Thus, we have developed numerical models in combination with experimental procedures so as to assess the potential maximum University of Utah TRIGA power with the currently available control rod system and have created feasibility studies for assessing new core configurations that could provide higher core power levels. For the maximum determined power of a new University of Utah TRIGA core arrangement, a new control rod system was proposed.

*Key words:* TRIGA, research reactor, control rod system, MCNP5 code

## INTRODUCTION

The university of Utah 100 kW TRIGA reactor (UUTR) was re-licensed on October 31, 2011, to operate for the next twenty years [1] at the maximum power level of 100 kW. Usually, we operate the reactor at the maximum power output of 90 kW. For the past two years, the use of UUTR was expanded to a wide range of experiments such as, but not limited to, various materials sample irradiation, neutron activation analysis (NAA), studies on irradiation damage to electronics materials, switches and devices, as well as fundamental experiments pertaining to biological and medical studies. A higher reactor power would open up some new opportunities for expanding the current use of the reactor's facility. A higher reactor power providing a higher neutron flux density would shorten the irradiation time of samples during NAA and material irradiations and would provide opportunities for designing new experiments such as, but not limited to: fast neutron studies, new types of experiments pertaining to material science and engineering, fast NAA, new biological and medical studies.

In this paper, we present a summary of extensive studies aimed at assessing the maximum achievable

UUTR core power with the available fuel elements in respect to the control rod system design. Part II of this paper is related to the assessment of the existing cooling system in respect to an UUTR power upgrade. When combined, these two studies have provided us with a basic design for a reactor power upgrade and expected associated costs. The main summary of the combined findings will be given in Part II of this paper. The impact of a possible power upgrade on the UUTR fuel burn-up rate and fuel management was not assessed in the article.

## UUTR CONTROL ROD SYSTEM

UUTR control rods (safety, shim and regulating) are made of aluminum clad boron carbide; each control rod has its own driver (fig. 1) [2].

Control rod reactivity worth (CRRW) is a measure of the control rod's ability to absorb neutrons; the greater the CRRW, the more neutrons it will absorb. The dollar worth of each CRRW is determined by a rod drop experiment; such experiments are performed at least semiannually at the UUTR. At the beginning of the rod drop experiment, the CRRW of the control rod to be measured is fully withdrawn from the core. Then, the UUTR is brought up to the critical power of 1 kW

\* Corresponding author; e-mail: tatjana.jevremovic@utah.edu

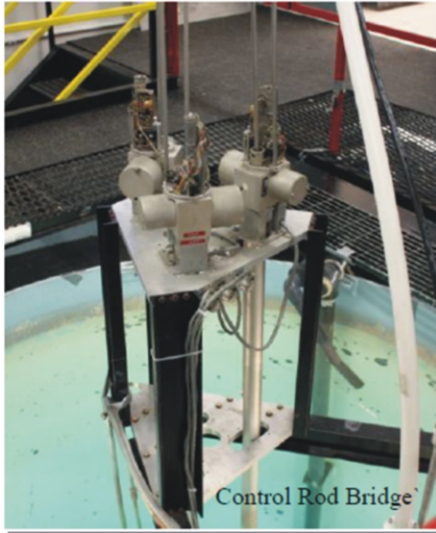


Figure 1. Current UTR control rod bridge [2]

which is high enough to allow the measurement of the CRRW. At the same time, this power level is low enough to neglect xenon poisoning and the effects of the temperature coefficient. This provides for the cold critical condition of the UUTR, meaning that the core is xenon-free, while both the fuel and the pool water temperatures are below 40 °C [3]. Once the power is stabilized at 1 kW, the magnetic disconnect switch holding the control rod is pressed, releasing only the measuring control rod into the core. The CRRW is, then, obtained by measuring the reactor period and by assessing the reactivity change through the in-hour equation [4, 5].

The MCNP5 code [6] is used to calculate the CRRW in the UUTR core.

There are two MCNP5 calculations that need to be performed in order to determine the CRRW of each control rod. The first calculation is related to the  $k_{\text{eff}}$  eigenvalue of the system when the control rod is fully withdrawn; the second is aimed at obtaining the  $k_{\text{eff}}$  eigenvalue of the system when the control rod is fully inserted into the core [7]. The change in reactivity determines the CRRW as

$$\text{CRRW}(\$) = \frac{k_2 - k_1}{k_2 k_1 \beta_{\text{eff}}} \quad (1)$$

where CRRW(\$) is the dollar control rod reactivity worth (the dollar is a unit equal to the change in reactivity needed to go from critical to prompt critical),  $k_2$  – the effective neutron multiplication factor when the control rod is fully withdrawn from the core,  $k_1$  – the effective neutron multiplication factor when the control rod is fully inserted into the core, and  $\beta_{\text{eff}}$  – the effective delayed neutron fraction.

The delayed neutron fraction  $\beta_{\text{eff}}$  is derived by the following equation

$$\beta_{\text{eff}} = 1 - \frac{k_p}{k_{\text{eff}}} \quad (2)$$

Table 1. Experimentally measured, MCNP5 calculated CRRW for UUTR operated at 90 kW

Control rod reactivity worth [\$]	Experiment		MCNP5	
Safety	2.254	0.166	1.911	0.021
Shim	1.513	0.119	1.450	0.017
Regulating	0.274	0.023	0.298	0.008
Total rod worth	4.041	0.308	3.658	0.046
Shutdown margin	1.005	0.102	0.823	0.009
Excess reactivity	0.794	0.127	0.950	0.009

where  $k_p$  is the computed eigenvalue contributed by prompt neutrons only, while  $k_{\text{eff}}$  – the computed eigenvalue contributed by both prompt and delayed neutrons. In addition, the  $\beta_{\text{eff}}$  – the calculated value is experimentally confirmed and recorded semiannually at the UUTR through the control rod drop experiment. In this paper, the  $\beta_{\text{eff}}$  value is 0.00774 [1, 8, 9].

The MCNP5-calculated UUTR CRRW for the current UUTR core is shown in tab. 1, in comparisons to experimental data [8, 9]. The relative error in CRRW measurements is derived by the standard deviation of all control rod measurements for the past ten years. The error in the MCNP5 calculated  $k_{\text{eff}}$  eigenvalue is the stochastic error associated with the Monte Carlo sampling method and is given alongside the result of the MCNP5 calculations as  $k_{\text{eff}}$  error. The values obtained are in good agreement with previous, measured, and computational errors.

The integral CRRW of each control rod is given as [10, 11]

$$\rho(\$) = A \sin^2 \frac{\pi x}{2H} = A \sin^2 \frac{\pi(\% \text{OUT})}{2} \quad (3)$$

where  $\rho(\$)$  is the cumulative reactivity inserted,  $A$  – the total reactivity worth of the control rod,  $x$  – represents the position of the control rod,  $H$  – the total height of the control rod, while %OUT represents the percentage of the control rod withdrawn from the core. Figure 2 shows the integral CRRW for the three control rods in the UUTR. As a function of the control rod position, each control rod contributes to dollar worth reactivity inserted into the reactor. 100% OUT means that the corresponding control rod is fully withdrawn from the reactor core, while 0% OUT corresponds to the control rod being fully inserted into the reactor. The curves showing the expected “S”-type shape are used to determine the reactivity change due to the movement of control rods between different positions, thus specifying the safety margin of the reactor.

Control rod interference, also known as the control rod shadowing effect, has been considered and evaluated and found to be negligible by our study [12].

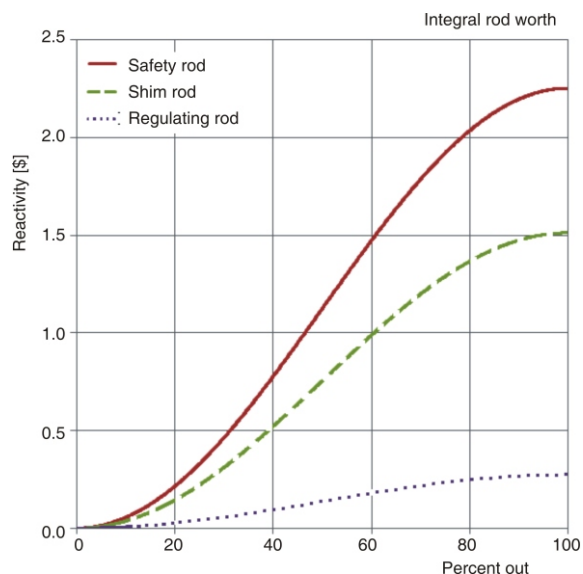


Figure 2. Calculated integral CRRW for the safety, shim, and regulating control rods in the UUTR by use of eq. (3)

### MAXIMUM ACHIEVABLE UUTR POWER WITH THE EXISTING CONTROL ROD SYSTEM AND CORE CONFIGURATION

A total of five experiments were performed to confirm and validate the relationship between the reactivity insertion and reactor power [8] and to validate the integral control rod curve [13, 14]. The extrapolation of experimental data allows for the approximation of the maximum practical UUTR power with the existing control rod system and fuel core set-up [15].

Experimental measurements and MCNP5 calculations at the UUTR were performed at power levels between 1 kW and 90 kW [16]. Table 2 summarizes the measured reactivity in comparison to MCNP5 eigenvalues for each of the power levels. The position of each control rod is known at every power level; therefore, the exact reactivity inserted into the core is also known at each of the power levels and control rod positions (fig. 2). The cumulative reactivity inserted, which is the total reactivity inserted contributed by all of the control rods, is plotted vs. the reactor power and shown in fig. 3; when more positive reactivity is inserted into the reactor, the neutron population in the reactor increases, increasing in turn the reactor power. Positive reactivity insertion is the only way to increase the power of a reactor. This is accomplished by either raising the control rods or by adding more fuel.

MCNP5 values are benchmarked against experimental measurements as also shown in fig. 3, indicating very good agreements. After the trend between reactivity insertion and reactor power is confirmed, it is extrapolated to determine the maximum achievable power of the current UUTR control rod system and current core configuration. The maximum amount of

Table 2. Reactor power, control rod position, cumulative reactivity inserted, and  $k_{eff}$  eigenvalue of the UUTR. All values below the 90 kW reactor power were experimentally confirmed

	Reactor power [kW]	Control rod position [%OUT]			Cumulative reactivity inserted [\$]	MCNP5 $k_{eff}$ eigenvalue*
		Safety control rod	Shim control rod	Regulation control rod		
Experimental measurements	1	100	51.1	65.0	3.207	0.99968
	10	100	54.4	65.0	3.289	1.00032
	20	100	57.5	65.0	3.362	1.00081
	30	100	60.1	65.0	3.429	1.00139
	40	100	62.4	65.5	3.486	1.00178
	50	100	64.7	65.5	3.541	1.00216
	60	100	66.9	65.5	3.587	1.00250
	70	100	69.2	65.5	3.633	1.00291
	80	100	71.7	65.5	3.679	1.00314
	90	100	74.3	65.5	3.727	1.00360
Extrapolated values	100	100	77.4	65.0	3.778	1.00403
	110	100	80.8	65.0	3.827	1.00443
	120	100	84.5	65.0	3.876	1.00483
	130	100	90.6	65.0	3.931	1.00523
	140	100	99.0	72.0	3.980	1.00563
	150	100	99.0	99.0	4.035	1.00603

\*The relative error in  $k_{eff}$  eigenvalue is 0.00004. MCNP5 on a Pentium Core 2 Quad Q6600 with 450 million particles

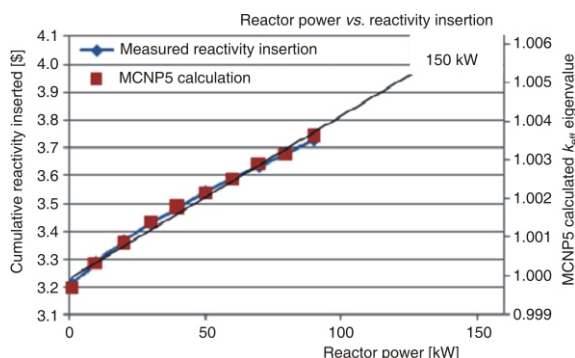


Figure 3. Maximum practical power of UUTR with the current control rod system

reactivity that can be inserted into the UUTR when all control rods are withdrawn is measured to obtain the value of \$4.041 (tab. 1). The highest  $k_{eff}$  eigenvalue calculated by withdrawing all control rods is 1.0065

0.00004. By linearly interpolating these values, the maximum achievable power for the UUTR is 150 kW with the currently existing control rod system and with no change in the current core configuration [15].

In addition, we show the analysis of fuel temperature coefficient trends. The fuel temperature coefficient is the change in reactivity per degree of change in fuel temperature [11, 15]. The UUTR has a negative fuel temperature coefficient, which means that the higher the fuel temperature, the more negative reactivity is inserted into the UUTR. This also becomes evident when referring to fig. 3 – the higher the power, the

more reactivity is required to be inserted into the core in order to increase the reactor power.

One of the advantageous safety features of the UUTR fuel is its strong negative fuel temperature coefficient [13] due to the uranium-zirconium-hydride (UZrH) fuel. When positive reactivity is added into the reactor through the withdrawal of control rods, the power of the reactor starts to increase [17]. As a result, fuel temperature increases. Simultaneously, the temperature of the zirconium-hydride (ZrH) increases. The high concentration of hydrogen mixed within the fuel increases the energy of the incoming neutrons (in other words, the up-scattering of neutrons is advanced) and therefore decreases the fission rate in the fuel. An increase in fuel temperature increases the probability that thermal neutrons will gain energy after interacting with the ZrH matrix and therefore escape out of the fuel rather than fission due to the increased mean free path for interaction [17]. This, in turn, decreases the power of the reactor and, thus, inherently controls the reactor. The fuel temperature coefficient can be obtained as [11]

$$\alpha = \frac{\Delta k}{K} \frac{d\rho}{dT} \frac{k_2}{k_2 k_1} \frac{k_1}{(T_2 - T_1)} \quad (4)$$

where  $\alpha$  is the reactivity coefficient expressed by the unit of  $\$/K$  in tabs. 3 and 4,  $\rho$  – the reactivity,  $T_1$  – the fuel temperature at  $k_1$ ,  $T_2$  – the fuel temperature at  $k_2$ ,  $k_1$  – the initial  $k_{\text{eff}}$  before the reactivity insertion, and  $k_2$  – the final  $k_{\text{eff}}$  after the reactivity insertion. Any amount of positive reactivity insertion into the reactor will result in an increase of reactor power. Hence, the reactor power is a function of the amount of reactivity inserted [3].

MCNP5 calculations are performed in order to numerically confirm the negative temperature coefficient trend for higher fuel temperatures [18]. The  $k_{\text{eff}}$  of the UUTR is calculated using ENDF/B-VII.1 neutron libraries at temperatures of 300 K, 600 K, 900 K, and 1200 K. The U-235, U-238, and Zr-H cross-section values which vary with temperature are taken into account through the  $S(\alpha, \beta)$  treatment [19]. The resulting  $k_{\text{eff}}$  is plotted vs. the fuel temperature [20]. The  $k_{\text{eff}}$  values correspond to all control rods out. Table 5 shows the MCNP5 calculated negative temperature coefficient vs. the temperature of the UUTR. MCNP5 calculations of the negative temperature coefficient correspond closely to the results of the UUTR safety analysis report [1]. All  $k_{\text{eff}}$  eigenvalue calculations are performed with 450 million particles on a Pentium Core 2 Quad Q6600.

It has been shown that UUTR power does not continually increase after positive reactivity has been inserted. In fact, reactor power starts to level off and stabilizes after fuel temperature is increased. This is because of the strong negative temperature coefficient of the UUTR fuel [22, 3]. The temperature coefficient

**Table 3. UUTR negative temperature coefficient of the C-4 fuel element**

Reactor power [kW]	Average cumulative reactivity inserted [β]	C-4 fuel pin temperature [°C]	$\Delta T_{C-4}$ [°C]	$\Delta \rho$ [β]	$\alpha_{C-4}$ [β/K]
1	3.207	27.2			
10	3.289	39.4	12.2	0.082	-0.00673
20	3.362	54.0	14.6	0.072	-0.00494
30	3.429	62.8	8.8	0.068	-0.00770
40	3.486	71.8	9.0	0.057	-0.00630
50	3.541	80.2	8.4	0.055	-0.00649
60	3.587	88.2	8.0	0.046	-0.00578
70	3.633	94.2	6.0	0.046	-0.00768
80	3.679	104.2	10.0	0.046	-0.00458
90	3.727	112.8	8.6	0.048	-0.00564

**Table 4. UUTR negative temperature coefficient of the D-11 fuel element**

Reactor power [kW]	Average cumulative reactivity inserted [β]	D-11 fuel pin temperature [°C]	$\Delta T_{D-11}$ [°C]	$\Delta \rho$ [β]	$\alpha_{D-11}$ [β/K]
1	3.207	27.8			
10	3.289	37.4	12.2	0.082	-0.00855
20	3.362	46.6	14.6	0.072	-0.00784
30	3.429	55.6	8.8	0.068	-0.00753
40	3.486	62.8	9.0	0.057	-0.00787
50	3.541	69.8	8.4	0.055	-0.00779
60	3.587	77.4	8.0	0.046	-0.00608
70	3.633	84.4	6.0	0.046	-0.00658
80	3.679	91.0	10.0	0.046	-0.00695
90	3.727	97.8	8.6	0.048	-0.00713

**Table 5. Summary of the UUTR average negative temperature coefficient**

$\alpha_{C-4}$ [β/K]	-0.00610	0.00115
$\alpha_{D-11}$ [β/K]	-0.00720	0.00066

can be obtained experimentally, by measuring the change in reactivity and dividing that value by the change in temperature as given in eq. (3). An increase in fuel temperature adds a negative amount of reactivity that is equal to the reactivity inserted into the reactor by the withdrawal of control rods. Table 3 and tab. 4 show the negative temperature coefficients of the two UUTR fuel elements we call fuel element “C-4” and fuel element “D-11”, respectively. The average negative temperature coefficients in these fuel elements are shown in tab. 5. The relationship between the fuel pin temperature and UUTR reactor power is linear for the measurements taken, as depicted in fig. 4. The effects of the fuel temperature coefficient become evident at temperatures above 40 °C, which is why fuel temperatures below 20 kW are not shown in this graph.

## ANALYSIS OF UUTR HIGHER POWER CORE CONFIGURATIONS

A gain of only 50 kW with the existing core arrangement and control rod system prompted us to ex-

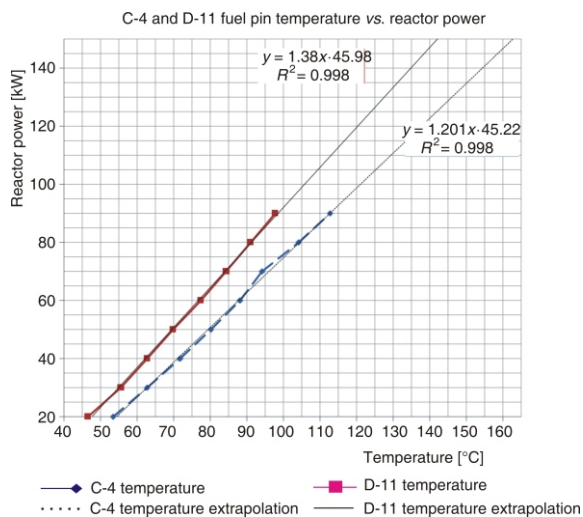


Figure 4. Fuel element temperature vs. reactor power

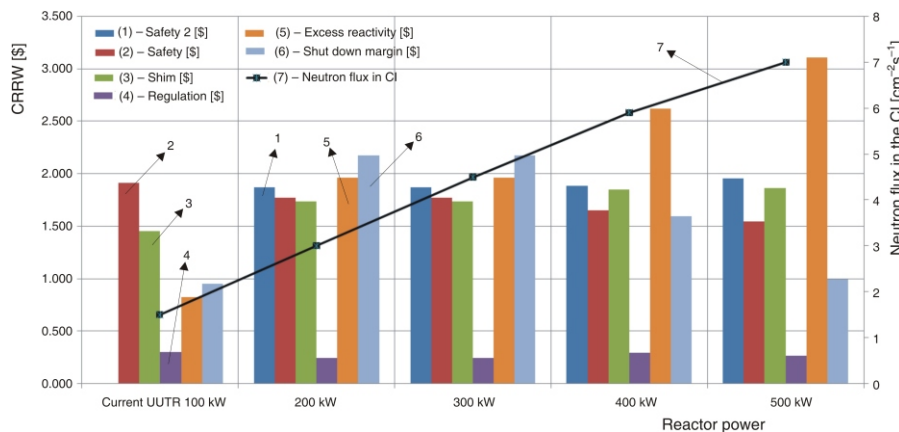
ment configurations resulting from the addition of fuel in order to increase the UUTR core power. Figure 5 summarizes the MCNP5 calculated CRRW for the “2” safety control rod, safety control rod, shim control rod, and regulating control rod. In addition, it shows the shutdown margin and excess reactivity, as well as the neutron flux density at the center of the core.

(b) *Power peaking factors.* The pin power ratio, which is the ratio between the fuel pin with the highest power and the average power per ring, is summarized in fig. 6. The power ratio  $P_f$  is calculated as [23]

$$P_f = \frac{P_{\max}}{P} \quad (5)$$

where  $P_{\max}$  is the highest power of the fuel pin and  $P$  is the average power per fuel ring. This ratio differs very slightly between different reactor designs because the neutron flux density per each reactor core is slightly

Figure 5. MCNP5 calculated CRRW and neutron flux density for each new UUTR power level



tend this study beyond the current configuration. Using the MCNP5 code, new UUTR core configurations are optimized for achieving higher power levels. Based on the existing core structure, four different reactor core designs were developed to provide power levels of 200 kW, 300 kW, 400 kW, and 500 kW. The design criteria we used to develop the new core arrangements for higher core power levels were: (a) to keep the shutdown margin of the new reactor core configurations equal or higher than that of the current UUTR core configuration, (b) to keep power peaking factors similar to the current core configuration, and (c) not to allow the neutron flux density shape across the reactor core to exhibit peaks and valleys when compared to the current UUTR core configuration.

(a) *Shutdown margin.* MCNP5 calculations have shown that an additional safety “2” control rod would be required for reactor powers above 150 kW. For higher powers, the safety “2” control rod becomes the control rod with the highest reactivity worth, because the flux density is higher around this control rod. The safety control rod also has a somewhat lesser reactivity worth for higher power reactor configurations, compared to the current one; this is due to different fuel ele-

different. In addition, for each specific reactor design, the peaking factors also differ per ring, because neutron flux density differs across the reactor core.

(c) *Neutron flux density distribution.* Concurrent with the reactor power upgrade, MCNP5 calculations are performed to confirm the negative temperature coefficient trend for higher fuel temperatures of higher

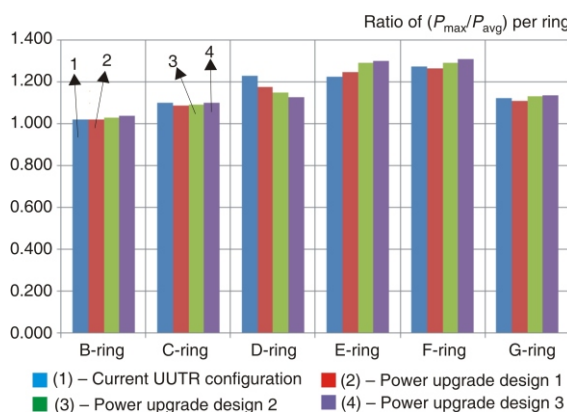


Figure 6. UUTR power ratio between the fuel pin with the highest power and average fuel pin power per ring

reactor powers of up to 500 kW. It was previously shown that there is a linear relationship between the fuel temperature and reactor power. However, the reactivity insertion for higher power levels will vary as a result of a non-linear fuel temperature coefficient. The  $k_{eff}$  of the UUTR is calculated in 50 kW increments from 100 kW to 500 kW. Table 6, tab. 7, and fig. 7 show the fuel pin temperature,  $k_{eff}$ , and the fuel temperature coefficient, respectively.

The linear trend between reactor power and fuel temperature is evident. In tandem, the fuel temperature coefficient shows to be decreasing for increasing reac-

**Table 6. UUTR C-4 fuel pin temperature,  $k_{eff}$ , and the fuel temperature coefficient**

Reactor power [kW]	MCNP5 calculated $k_{eff}$	C-4 fuel temperature [°C]	$\Delta T_{C-4}$ [°C]	$\Delta\rho$ ( $\Delta k/k$ )	$\alpha_{C-4}$ ( $\Delta k/K$ )
100	1.00404	121			
150	1.00610	162	41	0.00204	$-4.9661 \cdot 10^{-05}$
200	1.00820	204	42	0.00208	$-4.9453 \cdot 10^{-05}$
250	1.01036	245	41	0.00212	$-5.1226 \cdot 10^{-05}$
300	1.01257	287	42	0.00216	$-5.1978 \cdot 10^{-05}$
350	1.01482	329	42	0.00220	$-5.2085 \cdot 10^{-05}$
400	1.01713	370	41	0.00223	$-5.4731 \cdot 10^{-05}$
450	1.01949	412	42	0.00227	$-5.3901 \cdot 10^{-05}$
500	1.02189	453	41	0.00231	$-5.6577 \cdot 10^{-05}$

**Table 7. UUTR D-11 fuel pin temperature,  $k_{eff}$ , and the fuel temperature coefficient**

Reactor power [kW]	MCNP5 calculated $k_{eff}$	D-11 fuel temperature [°C]	$\Delta T_{D-11}$ [°C]	$\Delta\rho$ ( $\Delta k/k$ )	$\alpha_{D-11}$ ( $\Delta k/K$ )
100	1.00404	106			
150	1.00610	142	36	0.00204	$-5.6559 \cdot 10^{-05}$
200	1.00820	178	36	0.00208	$-5.7695 \cdot 10^{-05}$
250	1.01036	214	36	0.00212	$-5.8815 \cdot 10^{-05}$
300	1.01257	250	36	0.00216	$-5.9919 \cdot 10^{-05}$
350	1.01482	286	36	0.00220	$-6.1007 \cdot 10^{-05}$
400	1.01713	323	37	0.00223	$-6.0401 \cdot 10^{-05}$
450	1.01949	359	36	0.00227	$-6.3134 \cdot 10^{-05}$
500	1.02189	395	36	0.00231	$-6.4173 \cdot 10^{-05}$

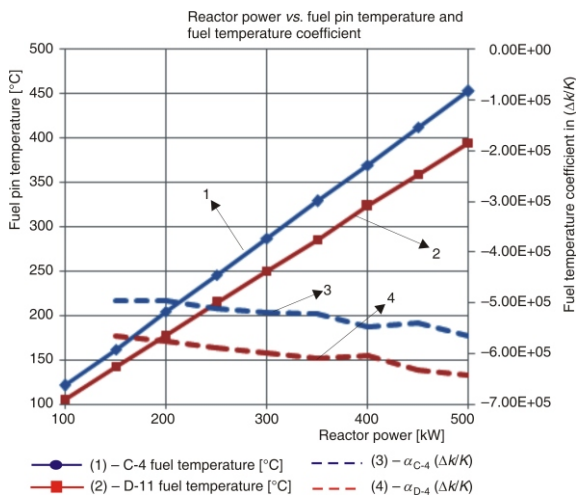


**Figure 7. UUTR power vs. fuel pin temperature and fuel pin temperature coefficient**

tor powers. This means that there is increasingly more reactivity insertion required for every incremental power increase. It is also evident that, in order to bring the reactor power from 100 kW to 150 kW, a 0.00204 ( $\Delta k/k$ ) of reactivity insertion is required. On the other hand, as reactor power increases, reactivity insertion increases as well. This is evident when increasing the reactor power from 450 kW to 500 kW, when a 0.00231 ( $\Delta k/k$ ) of reactivity insertion is required. This trend of an increasing negative temperature coefficient ensures the operational safety of the UUTR for higher reactor power levels.

UUTR pointwise thermal and fast neutron flux density [ $\text{cm}^{-2}\text{s}^{-1}$ ] distributions are shown in fig. 8 and fig. 9, respectively, while fig. 10 through fig. 17 show the difference in neutron flux density between 100 kW (current power) and 500 kW. The hexagonal outline represents the actual outline of the UUTR core. The general location where additional fuel elements were added for all UUTR powers above 150 kW is shown by the arrow pointer (fig. 10). It is evident from these figures that neutron flux density will increase proportionally to an increase in the reactor core power.

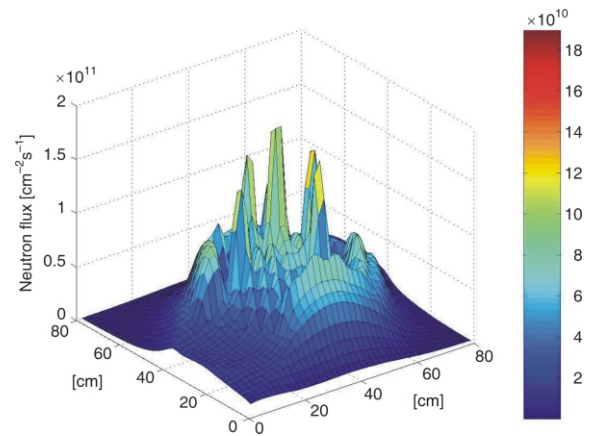


**Figure 8. 3-D thermal neutron flux density [ $\text{cm}^{-2}\text{s}^{-1}$ ] at 100 kW UUTR power for neutron energies below 25 meV**

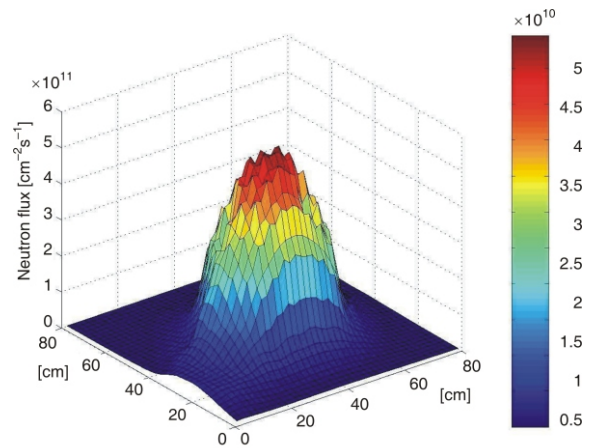


**Figure 9. 3-D fast neutron flux density [ $\text{cm}^{-2}\text{s}^{-1}$ ] at 100 kW UUTR power for neutron energies above 100 keV**

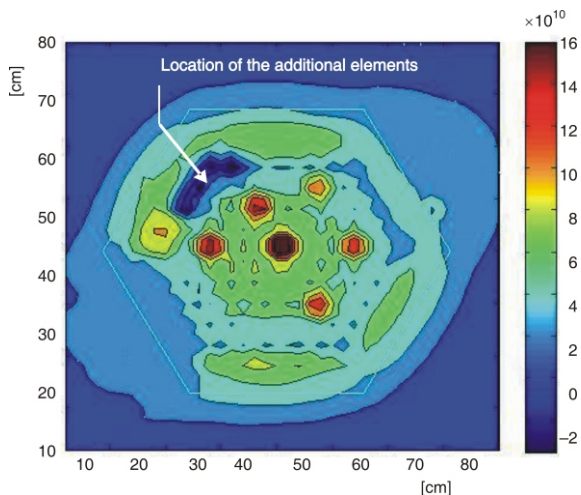


**Figure 10.** Top view of the core thermal flux density difference between 200 kW and 100 kW UTR power for neutron energies below 25 meV

Higher flux density means higher fission rates in the reactor, resulting in higher power. Another evident trend is that there is a substantial drop in the thermal neutron flux density at the location where additional fuel elements are added. It has been shown that thermal flux density decreases in the top left side of the core. Before the addition of the fuel, this location housed heavy water elements which moderated and reflected the neutrons back into the core. On the other hand, fast neutron flux density increases at the very same location (figs. 11, 13, 15, and 17). New fuel elements increase fission rates. This trend is evident for higher power levels, as well.

The UTR power ratio between the fuel pin with the highest power and the average fuel pin power per ring is shown in fig. 6. Power Upgrade Design 1 refers to the reactor power of 200 kW and 300 kW, Power Upgrade Design 2 refers to a 400 kW reactor power, while Power Upgrade Design 3 refers to 500 kW.

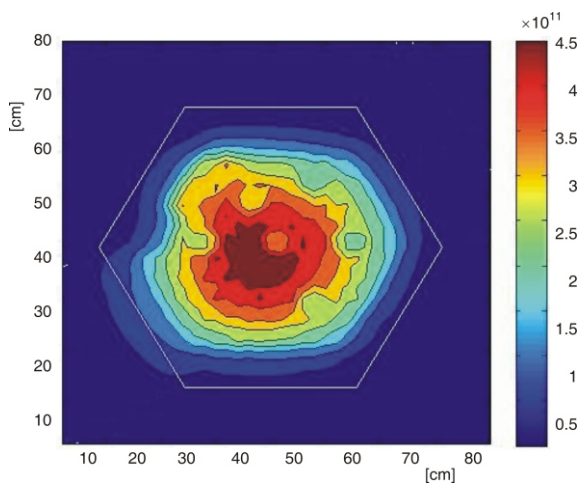


**Figure 11.** Top view of the core fast flux density difference between a 200 kW and 100 kW UTR power for neutron energies above 100 keV

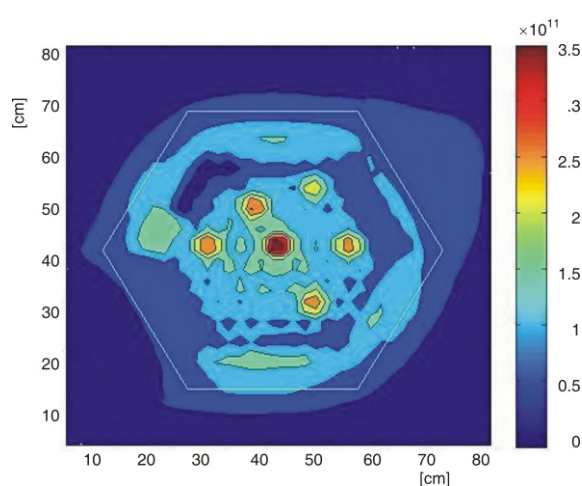


**Figure 12.** Top view of the core thermal flux density difference between the 300 kW and 100 kW UTR power for neutron energies below 25 meV

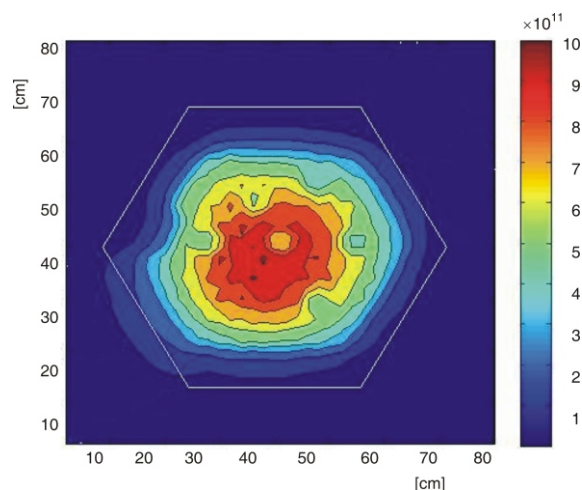


**Figure 13.** Top view of the core fast flux density difference between 300 kW and 100 kW UTR power for neutron energies above 100 keV

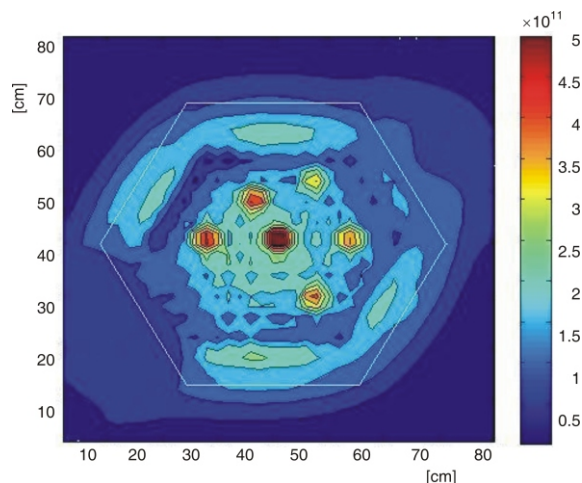


**Figure 14.** Top view of the core thermal flux density difference between 400 kW and 100 kW UTR power for neutron energies below 25 meV

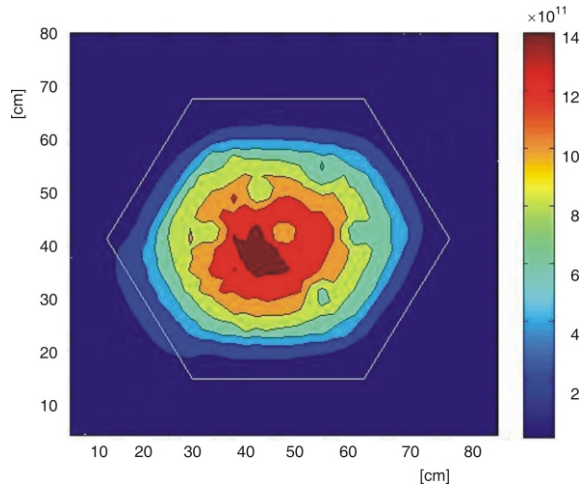


**Figure 15.** Top view of the core fast flux density difference between 400 kW and 100 kW UUTR power for neutron energies above 100 keV

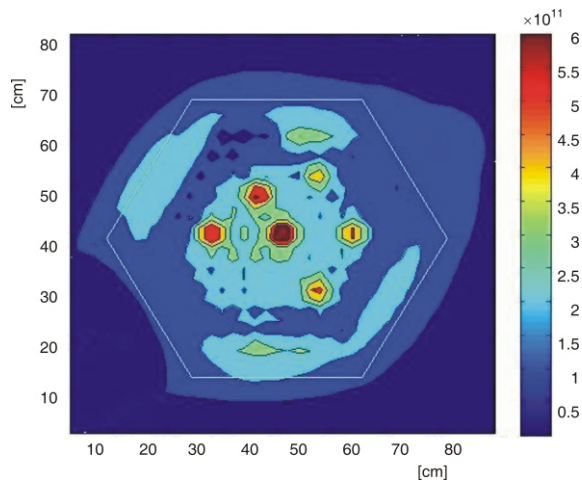


**Figure 16.** Top view of the core thermal flux density difference between 500 kW and 100 kW UUTR power for neutron energies below 25 meV

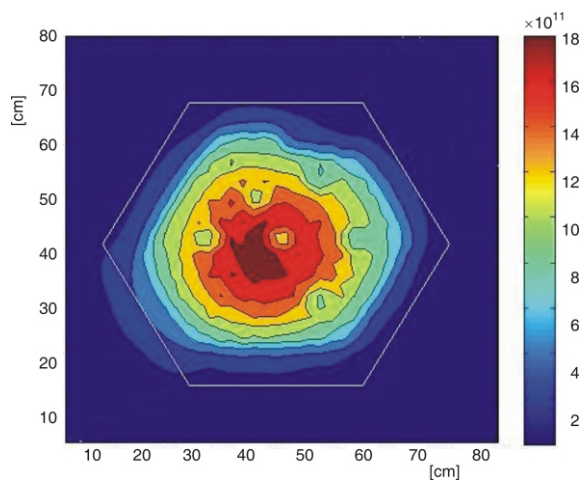


**Figure 17.** Top view of the core fast flux density difference between 500 kW and 100 kW UUTR power for neutron energies above 100 keV

The exact number of additional fuel elements is not stated; however, the number of fuel elements for design 1, 2, and 3, are  $1.05N$ ,  $1.08N$ , and  $1.15N$ , respectively, where  $N$  represents the number of fuel elements currently present in the UUTR.

## CONCLUSIONS

The presented neutronics-based feasibility study was the first of a two-part reactor core assessment of the UUTR. In the part at hand, in addition to core excess reactivity and the shutdown margin, the CRRW of each control rod of the current UUTR core was experimentally measured and numerically determined. Upon this, reactivity insertion contributed by each of the control rods was measured and assessed in order to determine the highest achievable power for the current UUTR core configuration. The highest achievable reactor power of the current UUTR was estimated to be 150 kW, *i. e.* only 50 kW above the licensed power level.

In order to determine the requirements regarding the control rod system for higher core powers, MCNP5 was used to assess the CRRW, fuel temperature coefficients and excess reactivity for power levels of 200 kW, 300 kW, 400 kW, and 500 kW. The shutdown margin of each new reactor design was determined to be higher or equal to the shutdown margin of the current UUTR core. The power peaking factors of each reactor design were compared to the current UUTR and confirmed to be similar. The neutron flux density shape for each power upgrade design did not exhibit any unwanted peaks or valleys across any reactor cores. In conclusion, four viable reactor power upgrade designs, along with a new control rod system, were assessed. Any power level above 150 kW requires the installation of a new control rod system. In Part II of this paper, we will provide the final conclusions of the feasibility study of UUTR core power upgrades.

## AUTHOR CONTRIBUTIONS

Theoretical analysis, computer simulations, and experiments were carried out by A. Cutic with the help of D. Choe and T. Jevremovic. All three authors took part in analyzing and discussing the results. The manuscript was written and the figures and tables were prepared by all three authors.

## REFERENCES

- [1] \*\*\*, University of Utah – Submission of Safety Analysis Report, Technical Specifications and Responses to NRC RAIs, 2010, Document #ML10321004
- [2] Bess, J. D., Designing A High-Flux Trap in the University of Utah TRIGA Reactor, M. Sc. thesis, University of Utah, USA, 2005

- [3] Kimura, C. Y., Reactor Physics Experiments on a TRIGA Mark One Reactor, M. Sc. thesis, University of Utah, USA, 1979
- [4] Varvayanni, M., Catsaros, N., Antonopoulos-Domis, M., Estimation of Irradiated Control Rod Worth, *Annals of Nuclear Energy*, 36 (2009), 11-12, pp. 1706-1710
- [5] Varvayanni, M., Savva, P., Catsaros, N., Control Rod worth Calculations Using Deterministic and Stochastic Methods, *Annals of Nuclear Energy*, 36 (2009), 11-12, pp. 1718-1725
- [6] \*\*\*, RSICC Computer Code Collection: MCNP5/MCNPX. Oak Ridge National Laboratory, 2012, <http://www-rsicc.ornl.gov/>
- [7] Kalcheva, S., Koonen, E., Improved Monte Carlo-Perturbation Method for Estimation of Control Rod Worth in a Research Reactor, *Annals of Nuclear Energy*, 36 (2009), 3, pp. 344-349
- [8] \*\*\*, Utah Nuclear Engineering Program, Internal Document, Reactor Operation Log Books #33, #34, #35, #36, #37, and #38, 2000-2012
- [9] \*\*\*, Utah Nuclear Engineering Program, Internal Document, UNEP-STL-Start up and Termination Procedures and Logs, 2000-2012
- [10] \*\*\*, Reed Robert Burn, Introduction to Nuclear Reactor Operations, Detroit Edison Company, University of Michigan, USA, 1988
- [11] \*\*\*, US Department of Energy, DOE Fundamentals Handbook, Nuclear Physics and Reactor Theory, DOE-HDBK-1019, 1993
- [12] Cutic, A., Feasibility Study of the University of Utah TRIGA Reactor Power Upgrade in Respect to Control Rod System, M. Sc. thesis, University of Utah, USA, 2012
- [13] \*\*\*, General Atomics. Kinetic Behavior of TRIGA Reactors, Document GA-7882, Conference on Utilization of Research Reactors, Mexico City, Mexico, 1967
- [14] Elmer, E. L., Nuclear Reactor Physics, Academic Press, 2008
- [15] Gacuci, D. G., Handbook of Nuclear Engineering, Springer, 2010
- [16] Noble, B., *et al.*, Experimental and MCNP5 Based Evaluation of Neutron and Gamma Flux in the Irradiation Ports of the University of Utah Research Reactor, *Nucl Technol Radiat*, 27 (2012), 3, pp. 222-228
- [17] Carew, J., Cheng, L. A., *et. al.*, Physics and Safety Analysis for the NIST Research Reactor, BNL-71695-2003-IR, Brookhaven National Laboratory, Upton, N. Y., USA, 2003
- [18] Duderstadt, J. J., Hamilton, L. J., Nuclear Reactor Analysis, John Wiley & Sons, 1976
- [19] Engle, W. W., Williams, L. R., Temperature and Void Reactivity Coefficient Calculations for the High Flux Isotope Reactor Safety Analysis Report, ORNL/TM-12386, Oak Ridge National Laboratory, Oak Ridge, Tenn., USA, 1994
- [20] Brown, F. B., Mosteller, R. D., Sood, A., Verification of MCNP5, Nuclear Mathematical and Computational Science, *Proceedings*, American Nuclear Society Mathematics & Computation Topical Meeting, Gatlinburg, Tennessee; American Nuclear Society; 2003
- [21] Choi, H., Roh, G., Park, D., Benchmarking MCNP and WIMS/RFSP Against Measurement Data – II: Wolsong Nuclear Power Plant 2, *Nucl Sci Eng.*, 150 (2005), 1, pp. 37-55
- [22] \*\*\*, Nuclear Data for The Calculation of Thermal Reactor Reactivity Coefficients, *Proceedings*, Advisory Group Meeting Organized By the International Atomic Energy Agency and Held in Vienna, 7-10 December, 1987
- [23] Dawahra, S., Khattab, K., Calculation of the Power Distribution in the Fuel Rods of the Low Power Research Reactor Using the MCNP4C Code, *Annals of Nuclear Energy*, 38 (2011), 12, pp. 2859-2862

Received on January 22, 2013

Accepted on June 12, 2013

**Авдо ЂУТИЋ, Донгок ЂЕ, Татјана ЈЕВРЕМОВИЋ**

**ПОВЕЋАЊЕ СНАГЕ ИСТРАЖИВАЧКОГ РЕАКТОРА НА  
УНИВЕРЗИТЕТУ У ЈУТИ**

**Део I: Анализа заснована на пројекту и захтевима контролног система**

У овом раду описани су резултати детаљних анализа повећања снаге истраживачког TRIGA реактора на Универзитету у Јути, заснованих на пројекту и захтевима контролног система реактора. Иако садашња снага реактора од 100 kW омогућује одличне услове за широки спектар експеримената од интереса за истраживања, ипак је спроведена анализа повећања снаге реактора са постојећим горивним елементима и постојећом конфигурацијом реактора. Оваква анализа захтева детаљне нумеричке прорачуне који су обављени и упоређени са експерименталним мерењима. Анализе су искључиво спроведене са гледишта реакторских параметара као што су критичност реактора, неутронски флуks и параметри постојећег контролног система, са циљем да се оптимизује конфигурација реакторског језгра и максимална снага реактора. У раду су приказане анализе оптимизоване конфигурације реакторског језгра са повећаном снагом реактора.

*Кључне речи: TRIGA, истраживачки реактор, контролни систем, MCNP5 програм*